Distribution and characteristics of microplastic deposits on sandy beaches: integrating GNSS positioning, μ-Raman spectroscopy, and unsupervised models

Abstract: This study conducts a comprehensive investigation of microplastic (MP) pollution along the São Paulo State coastline (Brazil). The primary sources of MPs are identified as inadequate plastic waste management and containment system failures in port and industrial areas. These pollutants not only compromise the natural beauty of the beaches but also negatively impact marine life by altering the physical and chemical characteristics of the beaches and impacting dependent ecosystems. The research utilized a five-step methodology comprising a geodetic survey, analysis of beach morphometric parameters, collection of beach sediments, μ-RAMAN spectrometry for polymer identification, and the application of multivariate statistical models. For MP sample collection, the coastline was divided into six segments (C1 to C6). The results indicated higher MP concentrations in C3 and C2, suggesting the influence of industrial and port activities. Various MP types, such as pellets, fragments, and fibers, exhibited distinct distribution patterns, likely due to their different sources, intrinsic properties like shape and density, and emission and deposition processes. The analysis for the entire São Paulo coast revealed that beaches with characteristics (intermediate profile and facing the southern quadrant) tend to accumulate more MPs. The predominance of polymers such as polyethylene and polypropylene reflect the influence of industrial products on marine pollution. This study highlights the complexity of MP dynamics in the coastal environment and underscores the importance of considering the physical characteristics of the beaches, the diversity of MP types, and local human activities. Identifying areas more prone to the accumulation of this emerging pollutant is critical for developing targeted environmental monitoring and remediation strategies, which align with the peculiarities of each coastal region and contribute to the Sustainable Development Goals related to ocean health (SDG – 14).
Keywords: Marine litter, plastic particles, coastal deposition, extreme events.

1. Introduction

The Santos estuary, encompassing the city and the Port of Santos, along with the industrial region of Cubatão, represents a critical area for microplastic (MP) pollution, especially pellets, along the São Paulo coast (Ferreira et al., 2021). Inadequate plastic waste management and failures in containment systems are the leading causes of the entry of this pollutant into the environment, particularly during production, transport, and transshipment processes in factories and port terminals (Balthazar-Silva et al., 2020; Moreira et al., 2016; Turra et al., 2014).

The intense port activity, combined with high population density and industrial concentration, makes this region a hub for the dispersion of MP (Jong et al., 2022). Ivar do Sul & Costa (2014) pointed out that on Brazilian beaches, a high concentration of MPs is correlated with the intensity of port and industrial activities, especially in the Southeast region. The impacts caused by this pollutant affect not only the aesthetics of the beaches but also marine life due to the ingestion of these particles by marine organisms, causing physical and chemical damage, reflecting the severity of the situation (Rochman et al., 2013).

The presence of this emergent pollutant on coastal beaches has been observed to detract from their intrinsic aesthetic value, thereby impacting the visual appeal and recreational quality of these environments (Borriello, 2023; Corbau et al., 2023). Its diminutive size and the challenge in detection contribute to a gradual yet significant visual deterioration of beach landscapes. This degradation is frequently attributed by non-expert observers to ineffective environmental management and a general decline in ecosystem health (Hartley et al., 2015). Furthermore, this phenomenon not only reduces the attractiveness of these areas to tourists but also raises concerns regarding the health and well-being of both visitors and the local wildlife (Botero et al., 2021; Costa et al., 2022; da Silva et al., 2022; Göktuğ, 2021).

From a physical perspective, MP alter the composition and physical characteristics of beach environments, with potential repercussions for coastal ecosystems and the organisms reliant on these habitats for survival (Fries et al., 2013). The presence of MPs modifies sediment porosity, thereby impacting the drainage and moisture retention capabilities of beach substrates. This change in the physical environment can influence temperature-dependent sex determination in certain species, such as crustaceans and marine turtles (Carson et al., 2011; Nelms et al., 2016).

Chemically, MP can absorb and concentrate organochlorine contaminants, which include polychlorinated biphenyls (PCBs), dichlorodiphenyltrichloroethane (DDT), Polycyclic Aromatic Hydrocarbons (PAHs) and MEHP (Mono-ethyl-hexylphthalate, degraded from Diethyl-hexyl-phthalate or DEHP) (Brighty et al., 2015; Hartley et al., 2015; Ogata et al., 2009; Teuten et al., 2009) residual plastic from the action of Ultraviolet (UV) rays and/or the process of mechanical abrasion (Harris, 2020) begins to release greenhouse gases such as methane and ethylene (Royer et al., 2018). These chemical compounds can concentrate and transport chemical contaminants to marine biota and, by extension, humans through the food chain (Chelsea M Rochman et al., 2013; Rochman et al., 2014; Smith et al., 2018).

Through the combined analysis of geodetic, geomorphometric, and meteoceanographic factors at a beach along the São Paulo coastline, Ferreira et al. (2021) demonstrated that factors such as coastal currents and storm events can influence the deposition patterns of MP. Therefore, identifying the most suitable zones for their accumulation and systematizing potential MP accumulation areas are critical considerations (Avio et al., 2017; Hidalgo-Ruz et al., 2012a; Kim et al., 2015; Van Cauwenberghe et al., 2015). This study aims to conduct a novel and extensive evaluation of the correlations and interdependencies between various parameters, including the abundance and characteristics of MP, such as their shape and polymer type, and morphometric variables like elevation, slope, and orientation of beach facades. The focus is on identifying and understanding the distribution of these deposits across approximately 880 kilometers of beaches along the São Paulo coast in São Paulo, Brazil.

2. Methods

To indicate locations susceptible to MP deposition (MP hotspots), the data collection and analysis can be divided into three stages: 1) fieldwork – sediments sampling and beach morphometric parameters (aspect, slope, and altitude) using GNSS positioning; 2) laboratory analysis – sieving (1 – 5 mm mesh) and μ-RAMAN spectrometry for the confirmation of polymeric properties; 3) exploratory multivariate techniques – analytical hierarchy process-gaussian (AHP-G) and correspondence analysis (CA) (Figure 1).

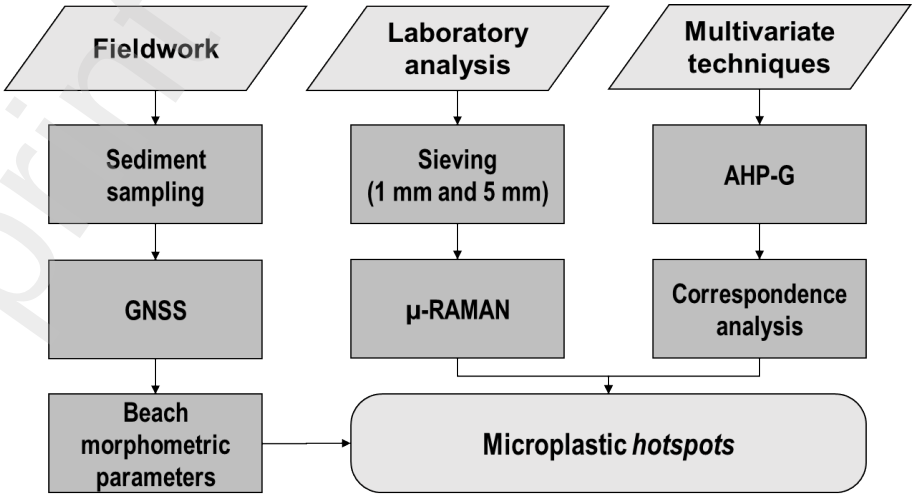

Figure 1. Flowchart summarizing the methods used in this research. GNSS: global navigation satellite system; AHP-G: analytical hierarchy process-gaussian.

2.1. Fieldwork

A complex interaction between geology, climate, and anthropic settings results in the varied coastal landscapes found in the state of São Paulo. The southern coast is dominantly low-lying, characterized by a wide coastal plain with extensive sandy beaches, lagoons and mangroves, including the Juréia-Itatins Ecological Station and Itinguçu State Park. Along the central and northern coasts, urbanization intensifies, and the Serra do Mar escarpment gradually approaches the coast, forming rocky headlands, pocket beaches and small islands (Souza, 2012; Tessler et al., 2018). This coast includes the city of Santos, where the largest port in Latin America is located. Ocean circulation is influenced by the warm Brazil Current flowing southward and the Brazil Coastal Current (Figure 2**a**), with coastal dynamics affected by the prevailing east-northeast winds and the stronger south-southeast winds, particularly during the winter (Campos et al., 1995; De Souza and Robinson, 2004; Möller Jr et al., 2008).

Sediment samples and beach morphology parameters were obtained along beach profiles distributed across all six compartments of the São Paulo coastline (Tessler et al., 2018), as shown in Table 1 and Figure 1**a**. The locations of sediment collection along each beach profile were selected based on environmental factors influencing litter dynamics on sandy beaches (GESAMP, 2019), particularly water levels. Sediment samples were obtained at four water levels (Figure 2**b**): storm strandline (P1), spring high tide (P2), neap high tide (P3), and low tide (P4). Each sample consisted of 500 g collected from the top layer of sediment within from 1 m² area (Figure 2f) at each of the 128 sampling points, yielding 1026 items identified as MP between 1 – 5 mm.

Table 1 – List of beach profiles per coastal compartment.

Compartment	Profiles ID	Number of profiles
C1 Ilha do Cardoso – Serra do Itatins	IC-A, IC-B, IC-C, IC-D, IC-E, IC-F	6
C2 Peruíbe – Praia Grande	PER, ITA, MON, PG	4
C3 Santos – Bertioga	GZN, ITR, GZG, GUA-A, GUA-B, TMB, AST, PIT-A, PIT-B, ENS-A, ENS-B, MCS, PEB	14
C4 Bertioga – Toque-Toque	BET, GRT, BOR	3
C5 Toque-Toque – Tabatinga	TOG, SSB, CRG, MSS	4
C6 Tabatinga – Picinguaba	UBA, ITB, PIC	3

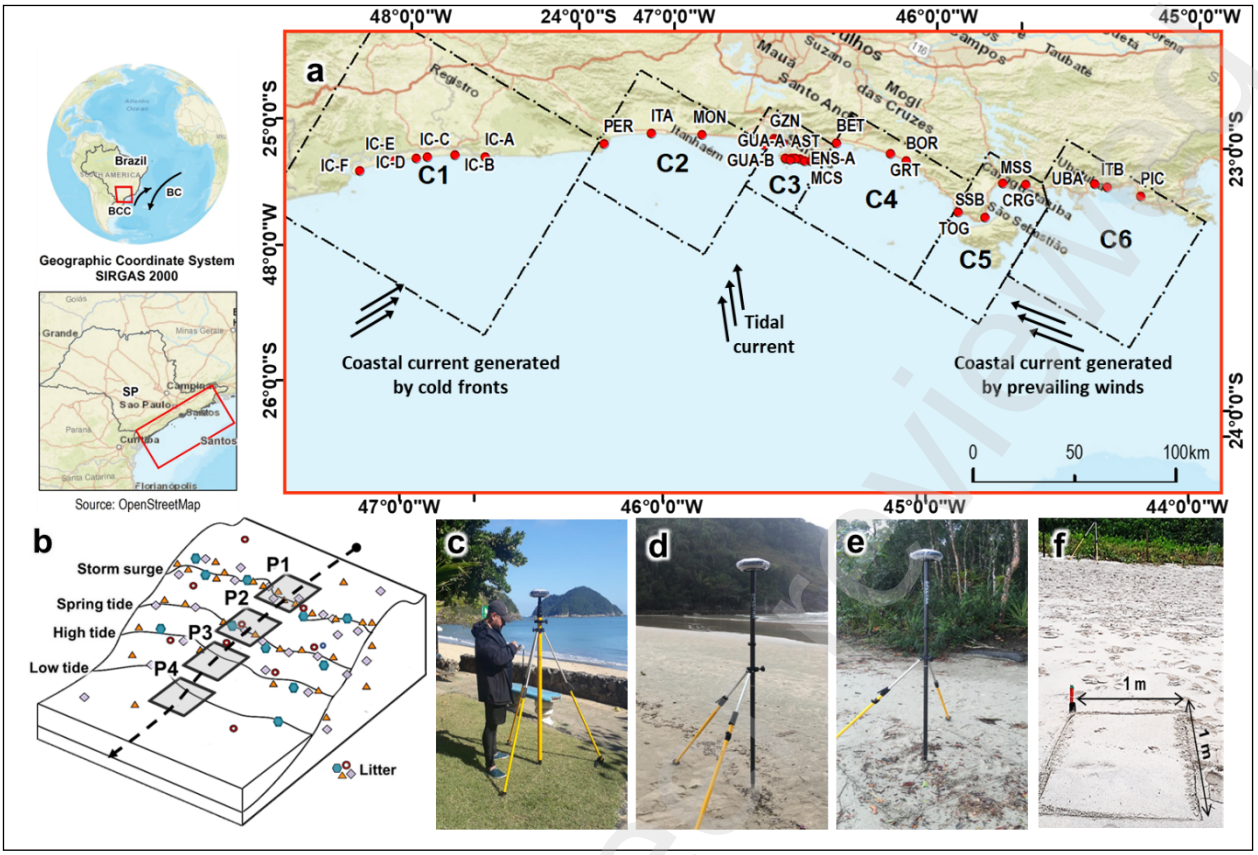

Figure 2 – (**a**) Sampling location distributed within the six compartments on the São Paulo coast. (BCC = Brazil Coastal Current, BC = Brazil Current), modified from Pianca et al. (2010); Tessler et al. (2018). (**b**) Sampling points by beach profile (P1, P2, P3, and P4), modified from GESAMP (2019); (**c**, **d**, and **e**) base, and GNSS Rovers; (**f**) area (1 m^2) of superficial sediment collection.

2.2. Morphometric parameters (GNSS)

The altimetry of the sampling points (P1, P2, P3, and P4) was obtained using the Global Navigation Satellite System (GNSS), following the method described in Ferreira et al. (2021). Reference stations were established within less than 5 km of markers distributed along the beach and positions were received from the nearest active stations of the Brazilian Network for Continuous Monitoring using the SIRGAS2000 coordinates system. Coordinates and altitudes of sampling points recorded by the mobile station were post-processed relative to the reference station (Monico, 2008; Monico et al., 2009) using the Survey Office software. The orthometric altitude (H) relative to the mean sea level of the Imbituba/SC datum of the Brazilian Geodetic System was obtained through Eq. 1 (Blitzkow et al., 2016):

$$H = h - N \quad (1)$$

where h is the geometric altitude obtained with GNSS referenced to the SIRGAS2000 ellipsoid, and N is the geoidal height determined by the IBGE geoidal model - MAPGEO2015. The altitudes (H) of the sampling points were classified according to Ferreira et al. (2021), as: Very Low (VL; < 1.42 m); Low (L; 1.42 – 1.57m); Mean (M; 1.58 – 1.89m); High (H; 1.90 – 2.06m); and Very High (VH; >2.06 m). The beach slope (tanβ) was derived from Eq. 2:

$$\tan\beta = \operatorname{atan}(VD/HD) \quad (2)$$

where VD and HD are the vertical and horizontal distances, respectively, between sampling points P1 and P4 (Figure 2b). The slope can be used as a proxy of the beach morphodynamic stage (Bujan et al., 2019), and can be categorized into steep (tanβ>0.12); intermediate (0.05 < tanβ < 0.12); and sloping (tanβ < 0.05) (Ferreira et al., 2023).

The aspect of the beach face is determined by the direction of the beach transect relative to the geographic north as follows (Burrough et al., 1998): North – N (0º - 22.5º); Northeast – NE (22.5º - 67.5º); East – E (67.5º - 112.5º); Southeast – SE (112.5º - 157.5º); South – S (157.5º - 202.5º); Southwest – SW (202.5º - 247.5º); West – W (247.5º - 292.5º); Northwest – NW (292.5º - 337.5º); North – N (337.5º - 360º).

2.3. Microplastic analysis

2.3.1. Sieving (surface samples)

The MP were extracted by sieving the samples using 1 – 5 mm mesh. The retained MP were visually separated from biological materials, such as shells, algae, and vegetation debris and subsequently identified, counted, and categorized according to shape (Löder and Gerdts, 2015): pellets (spherical or smooth), granular (foam), lines (fibers and filaments), and films (plastic film).

2.3.2. Polymeric characterization (μ-RAMAN spectrometry)

The polymeric characterization of MP was undertaken using μ-Raman spectroscopy (McCreery, 2005), using lasers with wavelengths of 473 nm, 532 nm, 633 nm, and 785 nm and a long-range 50x objective, numerical aperture (NA=0.55). First, the laser's power is calibrated to obtain ideal spectra in the polymer identification region (around 1600 cm^{-1}) to prevent damage to the materials. Subsequently, the analysis extends to the spectral region from 200 cm^{-1} to 3200 cm^{-1}, focusing on identifying hydrocarbons (Araujo et al., 2018; Ferraro, 2003; Smith and Dent, 2019). Additionally, adjustments in integration time, number of accumulations, and slit diameter are made to enhance the signal-to-noise ratio and avoid sensor saturation. A baseline is established for the acquired spectra, with subsequent noise filtering via a computational routine in Matlab®. Finally, the spectra are compared with the Knowitall® software database to identify polymer types. Concurrently, images of the MP are captured by the Raman system microscope, complementing the database.

2.4. Unsupervised models

Given the heterogeneous nature of the data (quantitative and qualitative variables), exploratory multivariate techniques such as analytical hierarchy process-gaussian (AHP-G) and correspondence analysis (CA) were employed (dos Santos et al., 2023; Fávero and Belfiore, 2017).

The AHP-G incorporates the Gaussian distribution to quantify and assess, through distributions, uncertainties in evaluations and probabilistic decision-making while maintaining the classic hierarchical structure of Saaty`s AHP (2008), without arbitrary weighting (Dos Santos et al., 2021; dos Santos et al., 2023). The result generates a ranking of MP abundance, subsequently standardized (Eq. 3) and transformed into a Likert scale (Table 2), allowing an assessment of the association between this ranking and beach morphometric parameters through CA.

The CA examines associations between variables of interest using the chi-square test (X^2; p-value < 0.05). In it, the Adjusted Standardized Residuals (ASR) check for dependence relationships between each variable based on the reference critical value (+1.96 ≤) of the standard normal curve for a 5% significance level. Thus, if the value of the ASR in a cell is greater than or equal to 1.96, it is interpreted that significant dependence relationships exist (Fávero and Belfiore, 2017; Haberman, 1978; Johnson and Wichern, 1992). All statistical analyses were performed in Anaconda/Spyder software using Python.

$$Standardization = \frac{(observed\ value)\ -\ (minimum\ value)}{(maximum\ value)\ -\ (minimum\ value)}$$

(3)

Table 2 – Standardized qualitative data based on the total count of polymers.

Ranking	Qualitative data
0.80 – 1.00	Very High (VH)
0.60 – 0.79	High (H)
0.40 – 0.59	Moderate (M)
0.20 – 0.39	Low (L)
0.00 – 0.19	Very Low (VL)

3. Results

3.1. Geographic distribution of microplastic

The majority of the 1,026 MP found consisted of fragments (42%) and foams (35%), with pellets, fibers, and films accounting for 20%, 3%, and 0.3%, respectively. Figure 3 shows the distribution of the standardized MP ranking across the study area. Low (L) and very low (VL) MP concentrations were found on beaches across all coastal compartments. In contrast, very high (VH) concentrations were predominantly found on beaches located in compartments C2 and C3 (PIT-B and ITA), with high (H) and moderate (M) concentrations identified in C4 and C1 (BOR and IC-D), respectively.

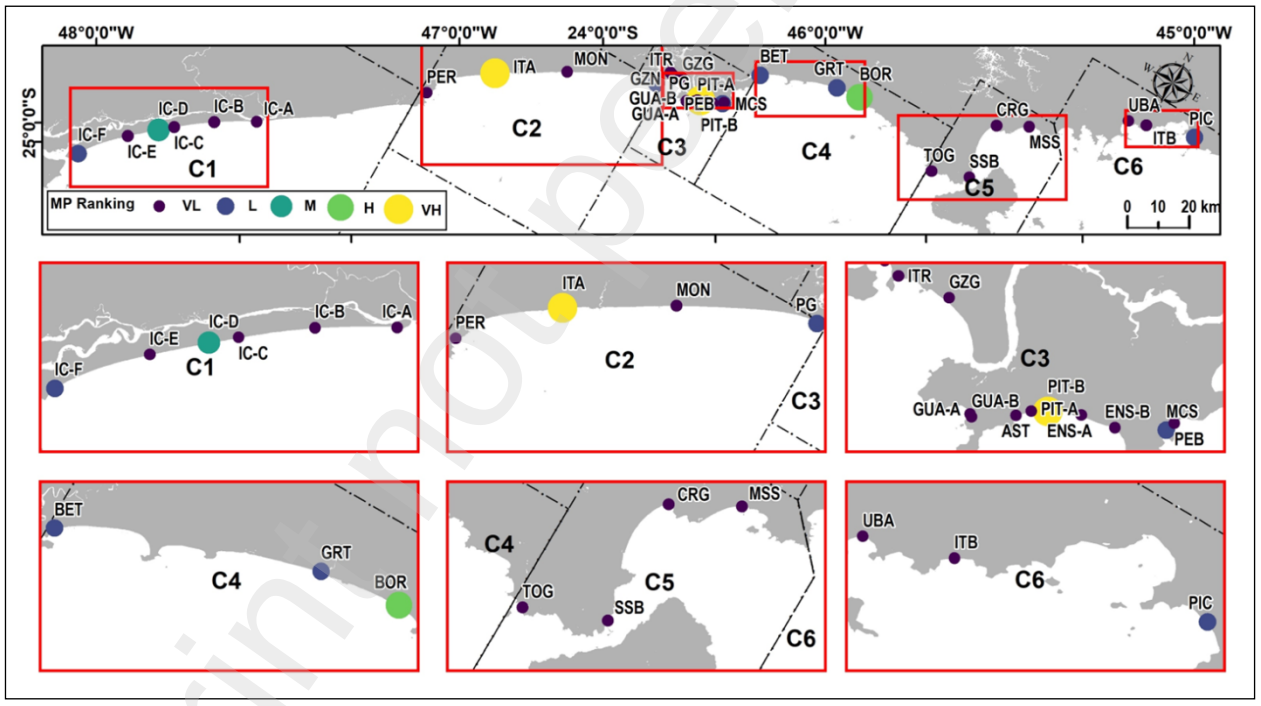

Figure 3 – MP ranking generated by the AHP-G method for the entire São Paulo coastline, highlighting compartments C1, C2, C3, C4, C5, and C6.

The X^2 statistical test indicated statistically significant associations ($p<0.05$) between the presence of all types of MP and the specific compartments in which they were found, except for films ($p=0.6885$). The CA identified a clear dependency relationship (ASR ≥1.96) between high (H) and very high (VH) MP concentrations and compartments C2 and C4, respectively. On the other hand, moderate (M), low (L), and very low (VL) concentrations were observed in compartments C1, C4, C3, and C5, in this order (Figure 4a). No significant relationship was found between MP concentrations and C6.

The concentration of pellets exhibited significant variations between compartments. Very high (VH) concentrations of pellets were significantly associated with beaches in C2 and C3 (Figure 4b). Significant associations were found between high (H) and very low (VL) concentrations of pellets in C1 beaches, with VL also found in C5. Moderate (M) concentrations were associated with beaches in C3 and C4, while low concentrations were significantly associated only with beaches in C6 (Figure 4b). Considering fragments, no significant association was found for VH concentrations, while H concentrations showed a significant relationship only with beaches in C3 (Figure 4c). Moderate concentrations of fragments were found to be significantly related to beaches in C2 and C4, with low concentrations associated with C3. Very low (VL) concentrations were significantly related to C1, C5, and C6. The presence of fibers showed no significant relationships with beaches in C5 and C6, while VH and VL concentrations were associated with beaches in C2 and C3, respectively, and moderate (M) concentrations wit beaches in C1 and C4 (Figure 4d). Similar to fibers, the presence of foam showed no significant relationships with C5 and C6. Significant associations were found between VH concentration of foam in C4, M in C2 and C3, and VL in C1 (Figure 4e). Films did not display significant dependency relationships with any compartment, although C3 exhibited the highest ARS values (Figure 4f).

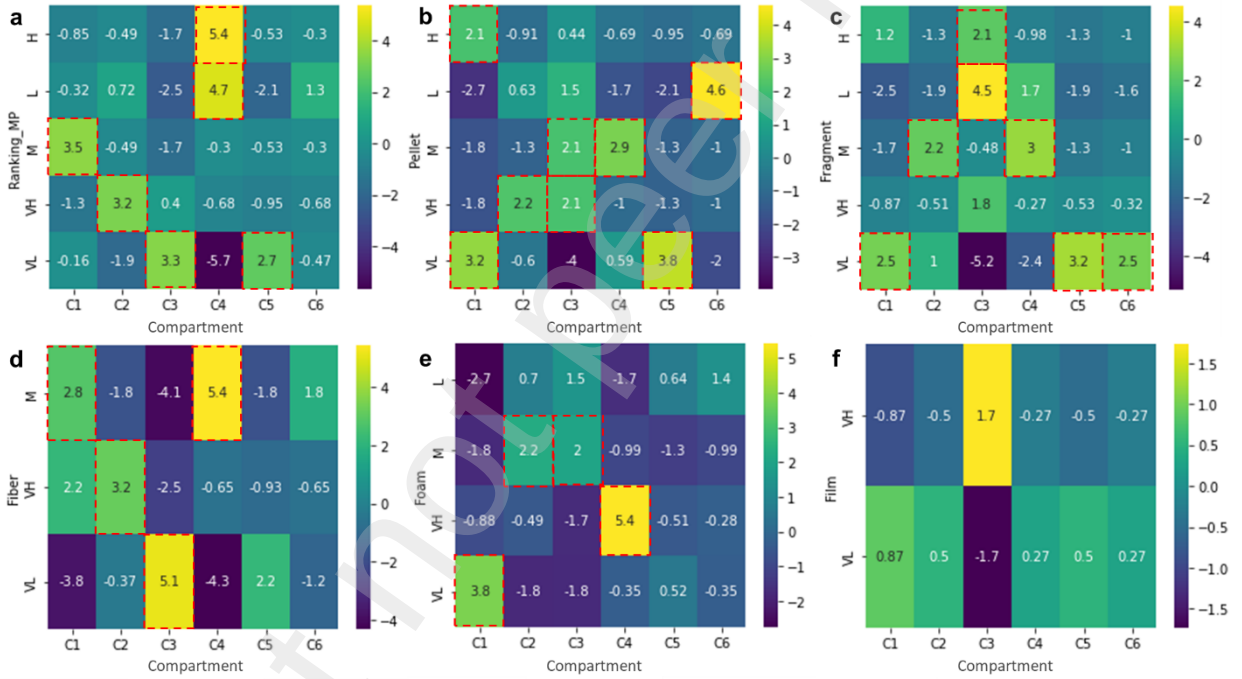

Figure 4 – Matrices showing the Adjusted Standardized Residual (ASR) values between the concentration rankings for MP (a), pellets (b), fragments (c), fibers (d), foam (e), and film (f) for each compartment (C1, C2, C3, C4, C5, and C6). Dashed red contours indicate variables exhibiting significant dependency relationships (ASR ≥ 1.96).

3.2. Associations between morphometric variables and microplastics

The X^2 test showed statistically significant associations between beach slope (tanβ p=2.2239E-07), aspect (p=1.1805E-06), and altitude (p=0.0016) and MP concentrations. Dependency relationships were identified between high MP concentrations and a southerly beach aspect (the slope faces the S quadrant), while low MP concentrations (L) were associated with an easterly beach aspect (Figure 5**a**). Very high and moderate MP concentrations showed a significant relationship with beach slopes classified as intermediate ($0.05 < \tan\beta < 0.12$) with low concentrations associated with gentler beach slopes ($\tan\beta < 0.05$), as illustrated in Figure 5**b**.

The analysis of ASR values indicated that very high MP counts along the beach profile are significantly related to high and very high altitudes (Figure 5**c**), reflecting strandlines along the upper parts of the beach profile (2.06 m to 2.62 m, above mean sea level). Conversely, very low MP concentrations were associated with very low altitudes (<1.90 m), suggesting strandlines along the lower part of the beach profile.

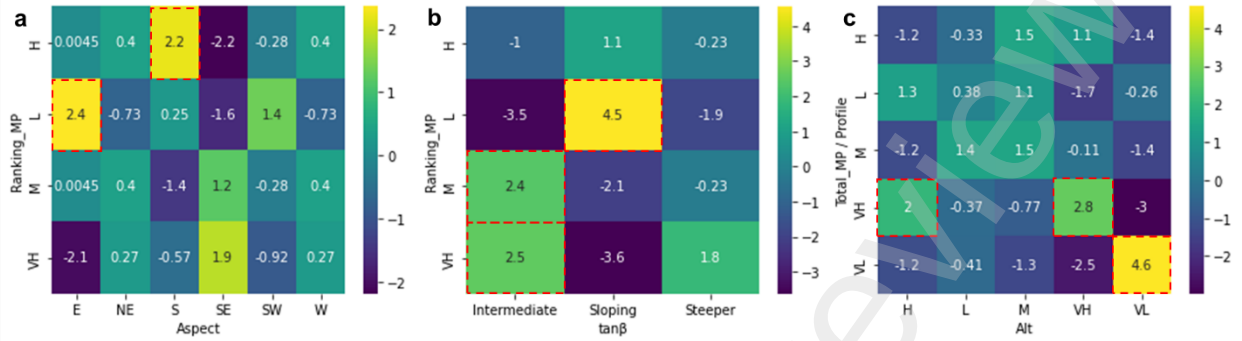

Figure 5 –Matrices showing the Adjusted Standardized Residual (ASR) values between MP rankings and the orientation of the beach face (Aspect) (**a**); beach slope (tanβ) (**b**), the total MP count per profile and the altitude (Alt) (**c**). Dashed red contours indicate significant relationships (ASR ≥ 1.96).

Results from the X^2 tests reveal that different MP types are more likely to be found at certain beach elevations, with significant associations ($p < 0.05$) found between altitude levels and pellets (p=1.6604E-10), fragments (p=0.0003), fibers (p=0.03677), foam (p=5.69E-08), and film (p=0.04353). Very high pellet concentrations were associated with very high altitudes (the upper beach), while low and moderate concentrations were significantly more prevalent in low and moderate altitudes, (Figure 6**a**). For fragments, high and very high concentrations were significantly associated with moderate altitudes (Figure 6b), with concentrations reducing in higher and lower beach elevations. Concentrations of fragments were very low at the lowest beach elevations, low at both high and low beach levels, and moderate at high and very high altitudes (Figure 6b). The accumulation of fibers showed a significant relationship only between moderate concentrations and very low altitudes (Figure 6**c**). Similar to fragments, very low concentrations of foam were significantly associated with very low altitudes and low concentrations were associated with high altitudes (Figure 6**d**). However, high and very high foam concentrations were found at the highest parts of the beach rather than at moderate altitudes as shown for fragments. Finally, very high film concentrations were associated with low altitudes, the only significant relationship found between this type of MP and altitude (Figure 6**e**).

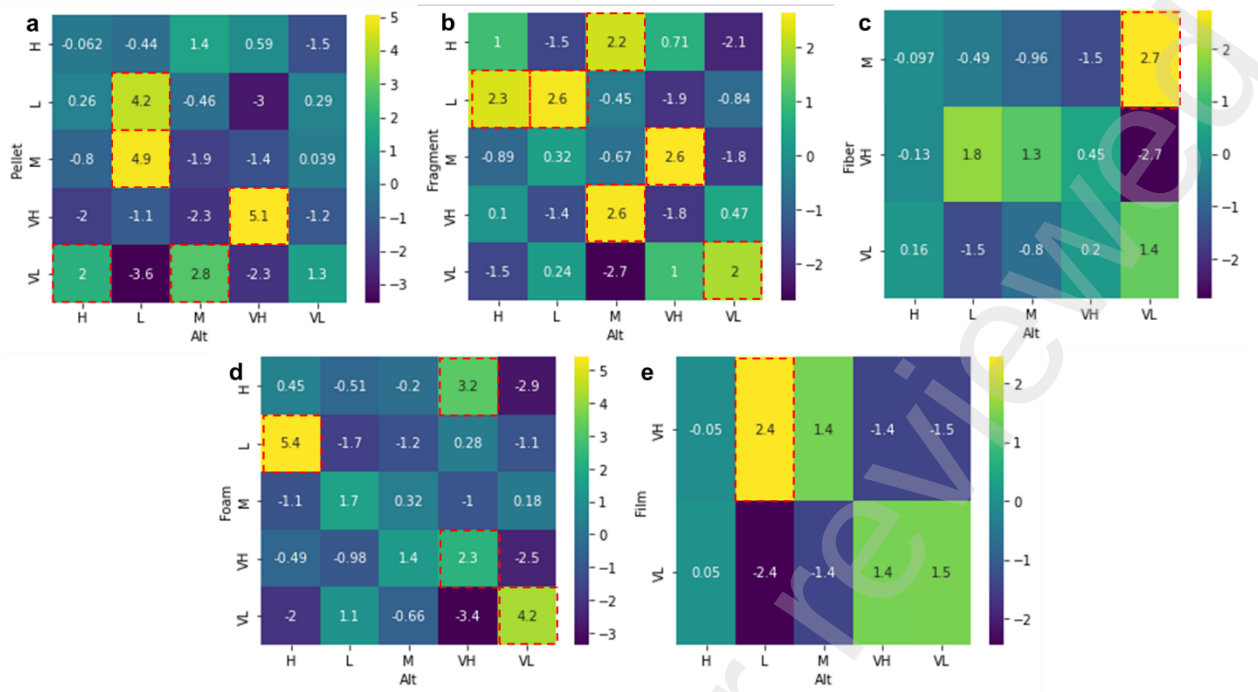

Figure 6 –Matrices of the Adjusted Standardized Residual (ASR) values between altitude (Alt) and the total count of pellets (**a**), fragments (**b**), fibers (c), foams (**d**), and films (**e**) per profile. Dashed red contours indicate significant relationships (ASR ≥ 1.96).

3.3. µ-Raman analysis

At the sites where the highest MP concentrations were observed (beach profiles IC-D in C1, ITA in C2, PIT-B in C3, and BOR in C4, Figure 3), the µ-Raman analyses (Figure 7) indicated that most pellets found on the upper beach were primarily polymers derived from high (HDPE) and low-density Polyethylenes (LDPE), along with other copolymers (Table 3). They were typically found in the form of small spherical or cylindrical granules, with HDPE exhibiting significant Raman peaks around 1130 cm^{-1}, 1295 cm^{-1}, and 1460 cm^{-1}, and a density range between 0.941 and 0.965 g/cm^3. LDPE showed Raman peaks similar to those of HDPE, maintaining the same characteristic peaks at 1130 cm^{-1}, 1295 cm^{-1}, and 1460 cm^{-1}, but with subtle differences in the spectral profile and a lower density range (0.910 to 0.940 g/cm^3).

The fragments and the fibers predominantly found at moderate altitudes in the beach profile exhibited the greatest diversity of polymeric material encountered. As they are derived from already industrialized products, these are commonly found in the form of polymers such as high and low-density Polyethylenes (HDPE and LDPE, respectively), identical to the pellets in Figures 7a and b, as well as Polypropylene (PP) (Figure 7c), and other copolymers including Ethylene-Polypropylene, Poly(Ethylene-co-Vinyl Acetate) , Poly(Propylene-Ethylene-Acrylic Acids), and High Ethylene Random Copolymer (RCP) (Table 1). PP is identified in the Raman spectrum by its distinct peaks at 841 cm^{-1}, 973 cm^{-1}, and 1160 cm^{-1}, with a density ranging between 0.855 and 0.946 g/cm^3.

Similarly to the fragments, foams also stood out for the diversity of their compounds. These polymers were predominantly identified and classified as Styrene (Figure 7d), including Polystyrene, Polyurethane, and Styrene/Allyl Alcohol Copolymer Low Molecular Weight (Table 2). Meanwhile, films primarily featured materials derived from polyethylene (Table 2). Styrene, a base monomer for polystyrene production, exhibits peaks in the Raman spectrum at 1000 cm^{-1}, 1030 cm^{-1}, and 1600 cm^{-1}. The density of polystyrene, a styrene derivative, is approximately 0.91 g/cm^3.

Table 3 – Main Polymers Identified by μ-Raman Spectrometry at different beach elevations (IC-D, ITA, PIT-B, and BOR).

Pellet	Fragment	Fiber	Foam	Film
High and Low Density Polyethylene	High and Low Density Polyethylene	High and Low Density Polyethylene	Styrene	Polyethylene
Poly(Ethylene), p-(Ethylene-co-Acrilyc-Acid)	Polypropylene		Polystyrene	
	Ethylene-Polypropylene		Polyurethane	
	Poly(Ethylene-co-Vinyl Acetate)		Styrene/Allyl Alcohol Copolymer Low Molecular Weight	
	Poly(Propylene-Ethylene-Acrylic Acids)			

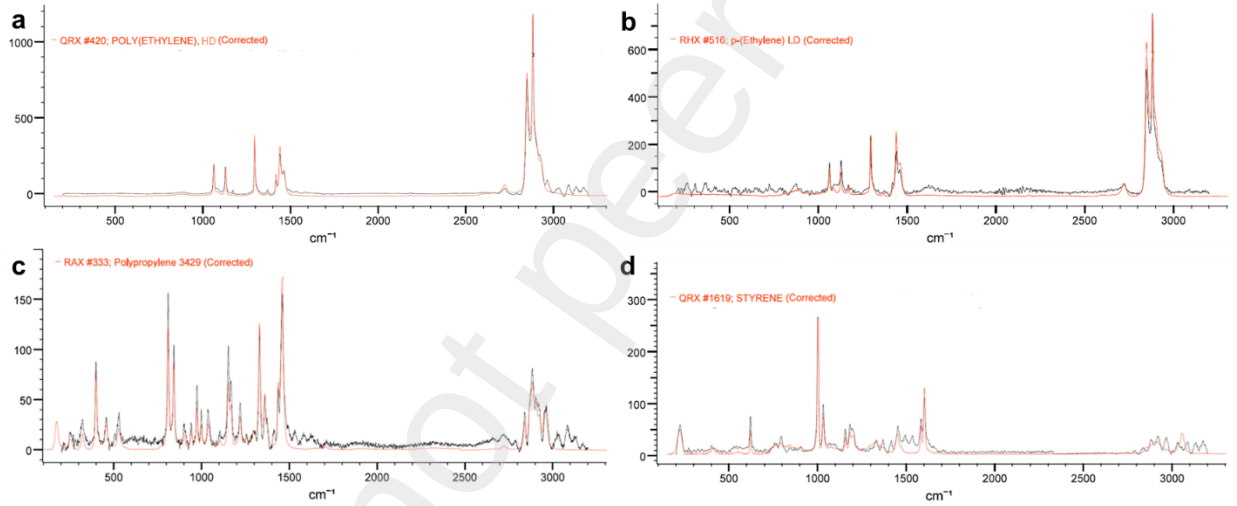

Figure 7 – Polymeric characterization by μ-Raman of the main polymers found in different sections of the beach profile: (**a** and **b**) High-Density and Low-Density Polyethylene (HDPE and LDPE, respectively); (**c**) Polypropylene; and (**d**) Styrene.

4. Discussion

The MP Ranking observed a distribution starting from the Santos Estuary and Mar Pequeno (São Vicente), initially depositing on beaches near these channels (e.g., sectors C3 and C2) and progressively accumulating as it moves toward the SSW, the same direction as the predominant coastal current in the region (NE-SW) (Tessler et al., 2018) on beaches such as Itanhaém (ITA) and those located on Ilha Comprida (IC-D), in sectors C2 and C1 of Figure 3, respectively. Conversely, beaches in sectors C4, C5, and C6 showed the lowest values in the Ranking. This suggests that beaches near Santos Bay are the first to be impacted due to their proximity to the primary sources of this pollutant, resulting from cities with higher population densities like Santos and São Vicente, in addition to the Port of Santos and the petrochemical industries in Cubatão. The latter two are responsible for the reception and processing of this material (Balthazar-Silva et al., 2020; Ferreira et al., 2021; Turra et al., 2014).

The analysis of the results on the distribution of MP across different compartments of the São Paulo coast provides a comprehensive overview of the environmental impact of this pollutant.

The applications of AHP-G, the χ^2 test, and AC have provided a robust statistical understanding of the distribution of these materials (Ferreira et al., 2023; Pereira et al., 2023; Santos et al., 2021).

Regarding different types of MP, the lack of a significant relationship for films suggests a distinct distribution dynamic or emission sources compared to other types of MP. This observation aligns with research indicating variations in sources and their environmental persistence (Tiwari et al., 2023).

The analysis of pellets and fragments shows significant dependence on specific compartments, indicating potential point sources of pollution or specific transport and deposition processes for these materials (Barnes et al., 2009; Lebreton et al., 2017). The high concentration of these materials in specific compartments (C3 and C2) underscores the need for more competent handling, transport, and manufacturing management (Tian et al., 2023). For fibers, the observed distribution suggests wide dispersion across different compartments, aligning with studies indicating their release from various sources, including the wear of synthetic fabrics and fishing nets (Oliveira et al., 2023; Zhang et al., 2022).

The results for foam are exciting, given the high dependency relation with compartment C4. This observation may be attributed to this material's specific characteristics or sources located near this compartment. On beaches, foam is commonly associated with waste from fishing materials or insulated containers for storing beverages and/or food, typically used by merchants and/or beachgoers (Chen et al., 2022; Zeng, 2023; Ziani et al., 2023).

The analysis of results regarding morphometric variables and their relationship with MP concentrations on beaches provides a relevant understanding of the distribution of this pollutant on the São Paulo coast and in the coastal environment. The χ^2 test and the analysis of RPA reveal statistically significant associations between the physical characteristics of the beaches and the presence of MP, aligning with previous studies that highlight the influence of geomorphological factors on the accumulation of marine debris (Ferreira et al., 2021; Hidalgo-Ruz and Thiel, 2013).

The relationship between the beach slope ($\tan\beta$) and the concentration of MP suggests that beaches with intermediate slope profiles are more prone to accumulate higher concentrations of MP, in general. This may be due to sediment and debris transport and deposition dynamics on these profiles (Andrady, 2011; Ferreira et al., 2021). Beaches with a dissipative trend ($\tan\beta < 0.05$) show lower concentrations. The flatter and lower profiles favor beach washing during high tides and, consequently, the fluctuation of MPs back into the coastal current (Cooper and McLaughlin, 1998; Ferreira et al., 2021). The orientation of the beaches (Aspect) also shows a significant relationship with the concentration of MP (Vito et al., 2022). Beaches facing the South quadrant exhibit higher concentrations in the same direction as the higher energy storm waves (Ferreira et al., 2021; Young and Elliott, 2018) come from this direction. According to Ferreira et al. (2023), beaches on the São Paulo coast with this orientation naturally accumulate sediments and marine litter.

Regarding altitude, the observed association between higher altitudes and higher MP concentrations can be attributed to the deposition of debris brought by high tide processes combined with storm events, which deposit material in higher areas of the beach (Álvarez-Hernández et al., 2019; Ferreira et al., 2021; Lavers and Bond, 2017; Schmuck et al., 2017; Young and Elliott, 2018). The distribution of pellets, fragments, fibers, foams, and films about altitude reinforces the idea that different types of MP have distinct distribution dynamics, possibly influenced by their physical characteristics and sources of origin (Hidalgo-Ruz et al., 2012b).

The chemical identification of MPs through the μ-Raman technique has provided a robust approach to characterizing these materials, as evidenced in similar studies (Löder et al., 2015; Löder and Gerdts, 2015; Silva et al., 2018). Beach profiles IC-D, ITA, PIT-B, and BOR showed the highest values in the MP Ranking, indicating a significant concentration of MP in these areas. The predominance of polyethylene pellets (PE), both high-density (HDPE) and low-density (LDPE), reflects a typical pattern in coastal pollution of the São Paulo coast. These polymers are

widely used for their versatility and low cost, commonly found in consumer products and packaging (Chen et al., 2022; Zeng, 2023; Ziani et al., 2023).

HDPE, LDPE, PP, and Styrene exhibit distinct characteristics crucial for their identification and analysis in the Raman spectrum. Due to its resistance and durability, HDPE, a widely used polymer, displays significant Raman peaks around 1130 cm^{-1}, 1295 cm^{-1}, and 1460 cm^{-1}, associated with C-C and CH oscillations and CH_2 bending. The density of HDPE varies between 0.941 and 0.965 g/cm^3, reflecting its high crystallinity. On the other hand, LDPE, characterized by its flexibility, shows Raman peaks similar to those of HDPE but with subtle differences in the spectral profile due to its more branched structure, maintaining the same characteristic peaks at 1130 cm^{-1}, 1295 cm^{-1}, and 1460 cm^{-1}. Its density, influenced by lower crystallinity, is in the range of 0.910 to 0.940 g/cm^3 (Brandrup et al., 1999; Katsara et al., 2022; Tarani et al., 2023).

The diversity of polymers found in fragments and fibers, including PE, PP, and various copolymers, suggests a variety of pollution sources. These materials are often derived from already industrialized and discarded products, reflecting the widespread use of plastics in modern society and the inadequacy of waste management systems (Gao et al., 2022; Geyer et al., 2017). The identified foams and films, mainly composed of styrene and other polymers such as polystyrene and polyurethane, are consistent with literature highlighting the presence of these materials in marine environments. The former (styrene and polystyrene) are commonly used in packaging and thermal insulation applications due to their lightness and resistance. Polyethylene, widely used as the primary material in the manufacture of plastic bags and packaging, represents one of the most significant sources of MP pollution in the marine environment (Gao et al., 2023; Gunawan et al., 2022; Katsara et al., 2022).

The accumulation of pellets in the higher portions of beach profiles is a phenomenon that can be attributed to a combination of physical and geomorphological factors (Ferreira et al., 2021). These pellets' spherical or cylindrical shape, along with their relatively low density (0.910 and 0.965 g/cm^3), plays a crucial role in their deposition and distribution on beaches. This enhances the transportation of these microplastics by ocean currents and, specifically, their mobilization by high-energy waves and winds. When high-energy waves strike the beaches, particularly during high tides and storm events, these microplastics are driven to the upper sections of the beach profiles. Moreover, the spherical or cylindrical shape of the pellets reduces friction with the sand and other beach materials, facilitating wind transport through rolling and/or saltation. Once in the higher areas of the beach profile, these MPs tend to be retained due to the decreased energy of these factors (waves, winds, and tides), where they end up depositing and accumulating (Alvarez-Zeferino et al., 2020; Ferreira et al., 2021; Ryan et al., 2009).

In contrast to pellets, fragments and fibers often exhibit faceted or irregular shapes, influencing their transport dynamics and deposition on beaches. These irregular shapes increase resistance to movement in this environment, limiting their ability to be transported to higher beach areas, especially under the influence of less intense winds and waves (Oliveira et al., 2023; Lefebvre et al., 2023; Zhang et al., 2022). Furthermore, the density of these MP, generally higher than that of pellets, also contributes to their accumulation in the mid-regions (P2 and P3) of the beach profile. Fragments and fibers tend to settle where wave and current energy diminish, but it is still sufficient to mobilize them. This intermediate zone of the beach profile typically corresponds to a balance between areas reached by high tides and the extent of significant aeolian transport (Andrady, 2011; Ferreira et al., 2021; Jambeck et al., 2015).

The accumulation of expanded foams and plastic films in higher concentrations in the lower parts of beach profiles (P4, primarily, and P3) can be attributed to specific characteristics of these materials and the environmental dynamics of beaches. Foam, commonly composed of polystyrene and polyurethane, has a cellular structure that endows low density and high buoyancy (Auta et al., 2017; Gao et al., 2023). This low density allows foam to be easily transported by water, particularly by waves. However, its voluminous structure and lightness contribute to these materials being

deposited in the lower parts of beach profiles, where wave energy is insufficient to carry them to higher areas. In contrast, plastic films are generally thin and flexible, facilitating their movement by wind and wave action. Nevertheless, their flat shape and larger surface area relative to weight mean they are easily trapped in the lower beach areas (P4), where wind and wave energy is lower. Additionally, plastic films can become entangled with natural debris or adhere to moist sand, reducing mobility. (Andrady, 2011; Barnes et al., 2009; Browne et al., 2011; Martin et al., 2017; Rochman et al., 2013; Thompson et al., 2004).

This way, based on the aspects raised (Aspect, tanβ, and Altitude), it is possible to state that the locations with greater susceptibility to MP accumulation or potential hotspots depend on intermediate beach profiles facing the South quadrant and locations with excellent coastline stability and/or accretion. This is due to the ~90° angle between storm waves formed by cold fronts coming from the same quadrant, resulting in the near cessation of sediment transport on these beaches, favoring the accumulation of sediments and anthropogenic debris, including MP (Ferreira et al., 2023, 2021; Harris, 2020; Jong et al., 2022; Laurino et al., 2023; Stein and Siegle, 2019). This is because relative stability at some beaches can favor such deposition (Veerasingam et al., 2020), as seen in those associated with slow accretion processes, such as sandy spits and areas protected by tombolos, respectively, in compartments C1 and C3 (Ferreira et al., 2023; Mahiques et al., 2016; Mascagni et al., 2018; Silva et al., 2021).

Due to the configuration of the São Paulo coastline (SW-NE), beaches facing SE are more susceptible to erosive processes, as the acute angle (~45°) of incidence of storm waves (South) can reach up to 4.0 m (Andrade et al., 2019; Ferreira et al., 2023, 2021; Stein and Siegle, 2020, 2019) during the austral autumn and winter (April to September), favoring maximum sediment transport capacity (Sousa et al., 2013). On erosive beaches, sand removal can expose buried layers containing MP, increasing their availability to the marine environment (Ranjani et al., 2022; Sun et al., 2021; Wang et al., 2021).

In this context, the seasonal incidence of storms and extreme events (increasingly frequent) on the São Paulo coast (Gramcianinov et al., 2023; Nunes et al., 2018) may alter the MP dynamics. During storms, the resuspension and redistribution of sediments can increase the mobility of this pollutant (Cheung and Not, 2023). Harris et al. (2021) and Lebreton et al. (2017) emphasize that estuaries are significant vectors for transporting MP to the sea, influenced by urbanization and human activities. Thus, areas near river mouths and estuarine channels, such as those in Santos, São Vicente, and Bertioga, are critical points for the entry of MP into the ocean.

5. Conclusions

This study presented a comprehensive examination of the distribution of various types of MP (categories: pellet, fragment, fiber, foam, and film) along the São Paulo coastline, taking into account morphometric characteristics (i.e., beach face orientation - aspect; slope - tanβ; and altitude) and meteo-oceanographic conditions, uncovering complex and significant patterns in the dispersion and accumulation of this pollutant. The findings, grounded in robust statistical analyses such as AHP-G, the X^2 test, and CA, ranked and indicated statistically significant associations between the presence of MP and specific geographic compartments and with the morphometric variables of the beaches. Notably, the highest concentrations of MP are predominantly found on compartments C3 and C2 beaches, suggesting a direct influence of proximity to urban and industrial sources, like the Santos Estuary and Mar Pequeno. The types of MP, including pellets, fragments, fibers, and foams, exhibit distinct patterns of dependency on these compartments, reflecting potential differences in emission sources and transport and deposition processes.

The observed relationship between the environmental characteristics utilized and MP provides a comprehensive understanding of these pollutants' accumulation dynamics. The association of higher altitudes with elevated MP concentrations suggests a significant role of high tide processes and storm surges in depositing debris in higher beach areas.

μ-Raman spectroscopy revealed the predominance of polymers such as polyethylene (PE) in high and low-density forms, polypropylene (PP), and styrene, highlighting the significant contribution of industrialized and consumer products to MP pollution. Identifying susceptible locations for MP accumulation or hotspots along the coastline, using remote sensing data and morphometric analyses, observed that certain areas are particularly prone to MP concentration. These hotspots are often associated with intermediate beach profiles facing the South quadrant and locations with greater stability or accretion of the shoreline, where aggradation processes favor the accumulation of anthropogenic debris, including MP.

The study further highlights the complexity of MP dynamics in the coastal environment, emphasizing the importance of considering both the physical characteristics of the beaches and local human activities to understand and manage this type of pollution. Moreover, the variability in MP types and their relationships with different beach environments points to the need for differentiated management approaches tailored to the specific characteristics of each coastal compartment and pollutant type. Therefore, future studies linking the results found here with information derived from orbital remote sensing could generate models capable of predicting and synoptically expanding all these aspects.

Understanding these distribution patterns is crucial for developing effective monitoring and environmental remediation strategies in the São Paulo coast and other similar coastal regions. This contributes to achieving Sustainable Development Goal 14 (Life Below Water), explicitly targeting goal 14.1 —to prevent and significantly reduce marine pollution, particularly from land-based activities, including marine debris (indicator 14.1.1 — density of plastic debris) by 2025 — and 14. a, which seeks, among other objectives, to enhance scientific knowledge, develop research capacities, and transfer technology to improve ocean health (https://sdgs.un.org/goals/goal14).

6. Acknowledgment

7. References

Álvarez-Hernández, C., Cairós, C., López-Darias, J., Mazzetti, E., Hernández-Sánchez, C., González-Sálamo, J., Hernández-Borges, J., 2019. Microplastic debris in beaches of Tenerife (Canary Islands, Spain). Mar Pollut Bull 146, 26–32.

Alvarez-Zeferino, J.C., Ojeda-Benítez, S., Cruz-Salas, A.A., Martínez-Salvador, C., Vázquez Morillas, A., 2020. Dataset of quantification and classification of microplastics in Mexican sandy beaches. Data Brief 33, 106473.

Andrade, T.S. de, Sousa, P.H.G. de O., Siegle, E., 2019. Vulnerability to beach erosion based on a coastal processes approach. Applied Geography 102, 12–19.

Andrady, A.L., 2011. Microplastics in the marine environment. Mar Pollut Bull 62, 1596–1605.

Araujo, C.F., Nolasco, M.M., Ribeiro, A.M.P., Ribeiro-Claro, P.J.A., 2018. Identification of microplastics using Raman spectroscopy: Latest developments and future prospects. Water Res 142, 426–440.

Auta, H.S., Emenike, C.U., Fauziah, S.H., 2017. Distribution and importance of microplastics in the marine environment: a review of the sources, fate, effects, and potential solutions. Environ Int 102, 165–176.

Avio, C.G., Gorbi, S., Regoli, F., 2017. Plastics and microplastics in the oceans: From emerging pollutants to emerged threat. Mar Environ Res 128, 2–11.

Balthazar-Silva, D., Turra, A., Moreira, F.T., Camargo, R.M., Oliveira, A.L., Barbosa, L., Gorman, D., 2020. Rainfall and Tidal Cycle Regulate Seasonal Inputs of Microplastic Pellets to Sandy Beaches. Front Environ Sci 8.

Barnes, D.K.A., Galgani, F., Thompson, R.C., Barlaz, M., 2009. Accumulation and fragmentation of plastic debris in global environments. Philosophical Transactions of the Royal Society B: Biological Sciences 364, 1985–1998.

Blitzkow, D., de Matos, A.C.O.C., Xavier, E.M.L., Fortes, L.P.S., 2016. MAPGEO2015: O novo modelo de ondulação geoidal do brasil. Revista Brasileira de Cartografia 1873–1884.

Borriello, A., 2023. Preferences for microplastic marine pollution management strategies: An analysis of barriers and enablers for more sustainable choices. J Environ Manage 344, 118382.

Botero, C.M., Tamayo, D., Zielinski, S., Anfuso, G., 2021. Qualitative and quantitative beach cleanliness assessment to support marine litter management in tropical destinations. Water (Basel) 13, 3455.

Brandrup, J., Immergut, E.H., Grulke, E.A., Abe, A., Bloch, D.R., 1999. Polymer handbook. Wiley New York.

Brighty, G.C., Jones, D., Ruxton, J., 2015. High-Level Science Review for ' A Plastic Oceans ' Film.

Browne, M.A., Crump, P., Niven, S.J., Teuten, E., Tonkin, A., Galloway, T., Thompson, R., 2011. Accumulation of microplastic on shorelines woldwide: sources and sinks. Environ Sci Technol 45, 9175–9179.

Bujan, N., Cox, R., Masselink, G., 2019. From fine sand to boulders: Examining the relationship between beach-face slope and sediment size. Mar Geol 417, 106012.

Campos, E., Miller, J., Müller, T., Peterson, R., 1995. Physical Oceanography of the Southwest Atlantic Ocean. Oceanography 8, 87–91.

Carson, H.S., Colbert, S.L., Kaylor, M.J., McDermid, K.J., 2011. Small plastic debris changes water movement and heat transfer through beach sediments. Mar Pollut Bull 62, 1708–1713.

Chen, S., Lin, D., Gao, G., Guan, J., Belver, C., Bedia, J., 2022. Sources, Aging, and Management of Coastal Plastics in Shanghai. Water Air Soil Pollut 233, 437.

Cheung, C.K.H., Not, C., 2023. Impacts of extreme weather events on microplastic distribution in coastal environments. Science of The Total Environment 904, 166723.

Cooper, J.A.G., McLaughlin, S., 1998. Contemporary multidisciplinary approaches to coastal classification and environmental risk analysis. J Coast Res 512–524.

Corbau, C., Lazarou, A., Buoninsegni, J., Olivo, E., Gazale, V., Nardin, W., Simeoni, U., Carboni, D., 2023. Linking marine litter accumulation and beach user perceptions on pocket beaches of Northern Sardinia (Italy). Ocean Coast Manag 232, 106442.

Costa, L.L., Fanini, L., Ben-Haddad, M., Pinna, M., Zalmon, I.R., 2022. Marine litter impact on sandy beach fauna: A review to obtain an indication of where research should contribute more. Microplastics 1, 554–571.

da Silva, E.F., do Carmo, D. de F., Muniz, M.C., Dos Santos, C.A., Cardozo, B.B.I., de Oliveira Costa, D.M., Dos Anjos, R.M., Vezzone, M., 2022. Evaluation of microplastic and marine debris on the beaches of Niterói Oceanic Region, Rio De Janeiro, Brazil. Mar Pollut Bull 175, 113161.

de Oliveira, C.R.S., da Silva Júnior, A.H., Mulinari, J., Ferreira, A.J.S., da Silva, A., 2023. Fibrous microplastics released from textiles: Occurrence, fate, and remediation strategies. J Contam Hydrol 104169.

De Souza, R.B., Robinson, I.S., 2004. Lagrangian and satellite observations of the Brazilian Coastal Current. Cont Shelf Res 24, 241–262.

Dos Santos, M., de Araújo Costa, I.P., Gomes, C.F.S., 2021. Multicriteria decision-making in the selection of warships: a new approach to the AHP method. International Journal of the Analytic Hierarchy Process 13.

dos Santos, V.R., Fávero, L.P.L., Moreira, M.Â.L., dos Santos, M., de Oliveira, L. de A., de Araújo Costa, I.P., de Oliveira Capela, G.P., Kojima, E.H., 2023. Development of a computational tool in the Python language for the application of the AHP-Gaussian method. Procedia Comput Sci 221, 354–361.

Fávero, L.P., Belfiore, P., 2017. Manual de Análise de Dados: Estatística e Modelagem Multivariada com Excel®, SPSS® e Stata®. Elsevier, Rio de Janeiro, RJ, Brasil.

Ferraro, J.R., 2003. Introductory raman spectroscopy. Elsevier.

Ferreira, A.T. da S., Oliveira, R.C. de, Ribeiro, M.C.H., Grohmann, C.H., Siegle, E., 2023. Coastal Dynamics Analysis Based on Orbital Remote Sensing Big Data and Multivariate Statistical Models. Coasts 3, 160–174.

Ferreira, A.T. da S., Siegle, E., Ribeiro, M.C.H., Santos, M.S.T., Grohmann, C.H., 2021. The dynamics of plastic pellets on sandy beaches: a new methodological approach. Mar Environ Res 163, 105219.

Fries, E., Dekiff, J.H., Willmeyer, J., Nuelle, M.-T., Ebert, M., Remy, D., 2013. Identification of polymer types and additives in marine microplastic particles using pyrolysis-GC/MS and scanning electron microscopy. Environ Sci Process Impacts 15, 1949–1956.

Gao, G.H.Y., Helm, P., Baker, S., Rochman, C.M., 2023. Bromine Content Differentiates between Construction and Packaging Foams as Sources of Plastic and Microplastic Pollution. ACS ES&T Water 3, 876–884.

Gao, Z., Wontor, K., Cizdziel, J. V, Lu, H., 2022. Distribution and characteristics of microplastics in beach sand near the outlet of a major reservoir in north Mississippi, USA. Microplastics and Nanoplastics 2, 10.

GESAMP, 2019. Guidelines for the monitoring and assessment of plastic litter in the ocean, GESAMP Reports & Studies.

Geyer, R., Jambeck, J.R., Law, K.L., 2017. Production, use, and fate of all plastics ever made. Sci Adv 3, e1700782.

Göktuğ, T.H., 2021. Visitor-Sourced Pollution and Esthetic Quality in the Coastal National Parks: Sample of Dilek Peninsula Büyük Menderes Delta National Park/Turkey. Coastal Management 49, 183–200.

Gramcianinov, C., Staneva, J., De Camargo, R., Silva Dias, P., 2023. Changes in extreme wave events in the southwestern South Atlantic Ocean. Ocean Dyn.

Gunawan, N.R., Tessman, M., Zhen, D., Johnson, L., Evans, P., Clements, S.M., Pomeroy, R.S., Burkart, M.D., Simkovsky, R., Mayfield, S.P., 2022. Biodegradation of renewable polyurethane foams in marine environments occurs through depolymerization by marine microorganisms. Science of The Total Environment 850, 158761.

Haberman, S.J., 1978. Analysis of qualitative data: Introductory topics. Academic Press, Incorporated, New York, NY, New York.

Harris, P.T., 2020. The fate of microplastic in marine sedimentary environments: A review and synthesis. Mar Pollut Bull 158, 111398.

Harris, P.T., Westerveld, L., Nyberg, B., Maes, T., Macmillan-Lawler, M., Appelquist, L.R., 2021. Exposure of coastal environments to river-sourced plastic pollution. Science of the Total Environment 769, 145222.

Hartley, B.L., Thompson, R.C., Pahl, S., 2015. Marine litter education boosts children's understanding and self-reported actions. Mar Pollut Bull 90, 209–217.

Hidalgo-Ruz, V., Gutow, L., Thompson, R.C., Thiel, M., 2012a. Microplastics in the marine environment: A review of the methods used for identification and quantification. Environ Sci Technol 46, 3060–3075.

Hidalgo-Ruz, V., Gutow, L., Thompson, R.C., Thiel, M., 2012b. Microplastics in the Marine Environment: A Review of the Methods Used for Identification and Quantification. Environ Sci Technol 46, 3060–3075.

Hidalgo-Ruz, V., Thiel, M., 2013. Distribution and abundance of small plastic debris on beaches in the SE Pacific (Chile): a study supported by a citizen science project. Mar Environ Res 87, 12–18.

Ivar do Sul, J.A., Costa, M.F., 2014. The present and future of microplastic pollution in the marine environment. Environmental Pollution 185, 352–364.

Jambeck, J.R., Geyer, R., Wilcox, C., Siegler, T.R., Perryman, M., Andrady, A., Narayan, R., Law, K.L., 2015. Plastic waste inputs from land into the ocean. Science (1979) 347, 768–771.

Johnson, R.A., Wichern, D.W., 1992. Applied multivariate statistical analysis, New Jersey.

Jong, M.-C., Tong, X., Li, J., Xu, Z., Chng, S.H.Q., He, Y., Gin, K.Y.-H., 2022. Microplastics in equatorial coasts: Pollution hotspots and spatiotemporal variations associated with tropical monsoons. J Hazard Mater 424, 127626.

Katsara, K., Kenanakis, G., Alissandrakis, E., Papadakis, V.M., 2022. Low-Density Polyethylene Migration from Food Packaging on Cured Meat Products Detected by Micro-Raman Spectroscopy. Microplastics 1, 428–439.

Kim, I.S., Chae, D.H., Kim, S.K., Choi, S.B., Woo, S.B., 2015. Factors Influencing the Spatial Variation of Microplastics on High-Tidal Coastal Beaches in Korea. Arch Environ Contam Toxicol 69, 299–309.

Laurino, I.R.A., Lima, T.P., Turra, A., 2023. Effects of natural and anthropogenic storm-stranded debris in upper-beach arthropods: Is wrack a prey hotspot for birds? Science of The Total Environment 857, 159468.

Lavers, J.L., Bond, A.L., 2017. Exceptional and rapid accumulation of anthropogenic debris on one of the world's most remote and pristine islands. Proc Natl Acad Sci U S A 114, 6052–6055.

Lebreton, L.C.M., Van Der Zwet, J., Damsteeg, J.-W., Slat, B., Andrady, A., Reisser, J., 2017. River plastic emissions to the world's oceans. Nat Commun 8, 15611.

Lefebvre, C., Le Bihanic, F., Jalón-Rojas, I., Dusacre, E., Chassaigne, L., Bichon, J., Clérandeau, C., Morin, B., Lecomte, S., Cachot, J., 2023. Spatial distribution of anthropogenic particles and microplastics in a meso-tidal lagoon (Arcachon Bay, France): A multi-compartment approach. Science of The Total Environment 898, 165460.

Löder, M.G.J., Gerdts, G., 2015. Methodology Used for the Detection and Identification of Microplastics—A Critical Appraisal BT - Marine Anthropogenic Litter. In: Bergmann, M., Gutow, L., Klages, M. (Eds.), . Springer International Publishing, Cham, pp. 201–227.

Löder, M.G.J., Kuczera, M., Mintenig, S., Lorenz, C., Gerdts, G., 2015. Focal plane array detector-based micro-Fourier-transform infrared imaging for the analysis of microplastics in environmental samples. Environmental Chemistry 12, 563–581.

Mahiques, M.M. de, Siegle, E., Alcántara-Carrió, J., Silva, F.G., de Oliveira Sousa, P.H.G., Martins, C.C., 2016. The Beaches of the State of São Paulo. In: Short, A.D., Klein, A.H.F. (Eds.), Brazilian Beach Systems. Springer, Berlin, Germany, pp. 397–418.

Martin, J., Lusher, A., Thompson, R.C., Morley, A., 2017. The Deposition and Accumulation of Microplastics in Marine Sediments and Bottom Water from the Irish Continental Shelf. Sci Rep 7, 1–9.

Mascagni, M.L., Siegle, E., Tessler, M.G., Y Goya, S.C., 2018. Morphodynamics of a wave dominated embayed beach on an irregular rocky coastline. Braz J Oceanogr 66, 172–188.

McCreery, R.L., 2005. Raman spectroscopy for chemical analysis. John Wiley & Sons.

Möller Jr, O.O., Piola, A.R., Freitas, A.C., Campos, E.J.D., 2008. The effects of river discharge and seasonal winds on the shelf off southeastern South America. Cont Shelf Res 28, 1607–1624.

Monico, J.F.G., 2008. Posicionamento pelo GNSS: descrição, fundamentos e aplicações, São Paulo. Editora UNESP, São Paulo.

Monico, J.F.G., Dal Poz, A.P., Galo, M., Dos Santos, M.C., De Oliveira, L.C., 2009. Acurácia e precisão: revendo os conceitos de forma acurada. Boletim de Ciências Geodésicas 15, 469–483.

Moreira, F.T., Balthazar-Silva, D., Barbosa, L., Turra, A., 2016. Revealing accumulation zones of plastic pellets in sandy beaches. Environmental Pollution 218, 313–321.

Nelms, S.E., Duncan, E.M., Broderick, A.C., Galloway, T.S., Godfrey, M.H., Hamann, M., Lindeque, P.K., Godley, B.J., 2016. Plastic and marine turtles: A review and call for research. ICES Journal of Marine Science 73, 165–181.

Nunes, L.H., Greco, R., Marengo, J.A., 2018. Climate change in Santos Brazil: Projections, impacts and adaptation options, Climate Change in Santos Brazil: Projections, Impacts and Adaptation Options.

Ogata, Y., Takada, H., Mizukawa, K., Hirai, H., Iwasa, S., Endo, S., Mato, Y., Saha, M., Okuda, K., Nakashima, A., Murakami, M., Zurcher, N., Booyatumanondo, R., Zakaria, M.P., Dung, L.Q., Gordon, M., Miguez, C., Suzuki, S., Moore, C., Karapanagioti, H.K., Weerts, S., McClurg, T., Burres, E., Smith, W., Velkenburg, M. Van, Lang, J.S., Lang, R.C., Laursen, D., Danner, B., Stewardson, N., Thompson, R.C., 2009. International Pellet Watch: Global monitoring of persistent organic pollutants (POPs) in coastal waters. 1. Initial phase data on PCBs, DDTs, and HCHs. Mar Pollut Bull 58, 1437–1446.

Peter A. Burrough, McDonnell, R.A., Lloyd, C.D., 1998. Principles of Geographical Information Systems. Oxford University Press, New York, NY, USA.

Pianca, C., Mazzini, P.L.F., Siegle, E., 2010. Brazilian offshore wave climate based on NWW3 reanalysis. Braz J Oceanogr 58, 53–70.

Ponçano, W.L., Tessler, M.G., Freitas, C.G.L. de, Mahiques, M.M. de, 1999. Tendências regionais de transporte de sedimentos arenosos ao longo das praias paulistas. Revista UNG. Geociências. Ano IV (6) 102, 120.

Ranjani, M., Veerasingam, S., Venkatachalapathy, R., Jinoj, T.P.S., Guganathan, L., Mugilarasan, M., Vethamony, P., 2022. Seasonal variation, polymer hazard risk and controlling factors of

microplastics in beach sediments along the southeast coast of India. Environmental Pollution 305, 119315.
Rochman, Chelsea M., Browne, M.A., Halpern, B.S., Hentschel, B.T., Hoh, E., Karapanagioti, H.K., Rios-Mendoza, L.M., Takada, H., Teh, S., Thompson, R.C., 2013. Policy: Classify plastic waste as hazardous. Nature 494, 169–170.
Rochman, Chelsea M, Hoh, E., Kurobe, T., Teh, S.J., 2013. Ingested plastic transfers hazardous chemicals to fish and induces hepatic stress. Sci Rep 3, 1–7.
Rochman, C.M., Kurobe, T., Flores, I., Teh, S.J., 2014. Early warning signs of endocrine disruption in adult fish from the ingestion of polyethylene with and without sorbed chemical pollutants from the marine environment. Science of the Total Environment 493, 656–661.
Royer, S.-J., Ferrón, S., Wilson, S.T., Karl, D.M., 2018. Production of methane and ethylene from plastic in the environment. PLoS One 13, e0200574.
Ryan, P.G., Moore, C.J., Van Franeker, J.A., Moloney, C.L., 2009. Monitoring the abundance of plastic debris in the marine environment. Philosophical Transactions of the Royal Society B: Biological Sciences 364, 1999–2012.
Saaty, T.L., 2008. Decision making with the analytic hierarchy process. International journal of services sciences 1, 83–98.
Schmuck, A.M., Lavers, J.L., Stuckenbrock, S., Sharp, P.B., Bond, A.L., 2017. Geophysical features influence the accumulation of beach debris on Caribbean islands. Mar Pollut Bull 121, 45–51.
Silva, A.B., Bastos, A.S., Justino, C.I.L., da Costa, J.P., Duarte, A.C., Rocha-Santos, T.A.P., 2018. Microplastics in the environment: Challenges in analytical chemistry-A review. Anal Chim Acta 1017, 1–19.
Silva, M.S., Guedes, C.C.F., da Silva, G.A.M., Ribeiro, G.P., 2021. Active mechanisms controlling morphodynamics of a coastal barrier: Ilha Comprida, Brazil. Ocean and Coastal Research 69, e21004.
Smith, E., Dent, G., 2019. Modern Raman spectroscopy: a practical approach. John Wiley & Sons.
Smith, M., Love, D.C., Rochman, C.M., Neff, R.A., 2018. Microplastics in Seafood and the Implications for Human Health. Curr Environ Health Rep 5, 375–386.
Sousa, P.H.G.O., Siegle, E., Tessler, M.G., 2013. Vulnerability assessment of Massaguaçú beach (SE Brazil). Ocean Coast Manag 77, 24–30.
Souza, C.R. de G., 2012. Praias Arenosas Oceânicas Do Estado De São Paulo (Brasil): Síntese Dos Conhecimentos Sobre Morfodinâmica, Sedimentologia, Transporte Costeiro E Erosão Costeira. Geography Department, University of Sao Paulo 307–371.
Stein, L.P., Siegle, E., 2019. Santos beach morphodynamics under high-energy conditions. Revista Brasileira de Geomorfologia 20, 445–456.
Stein, L.P., Siegle, E., 2020. Overtopping events on seawall-backed beaches: Santos Bay, SP, Brazil. Reg Stud Mar Sci 40.
Sun, X., Wang, T., Chen, B., Booth, A.M., Liu, S., Wang, R., Zhu, L., Zhao, X., Qu, K., Xia, B., 2021. Factors influencing the occurrence and distribution of microplastics in coastal sediments: from source to sink. J Hazard Mater 410, 124982.
Tarani, E., Arvanitidis, I., Christofilos, D., Bikiaris, D.N., Chrissafis, K., Vourlias, G., 2023. Calculation of the degree of crystallinity of HDPE/GNPs nanocomposites by using various experimental techniques: A comparative study. J Mater Sci 58, 1621–1639.

744 Tessler, M., Goya, S., Yoshikawa, P.H., 2018. S. Erosão e Progradação do Litoral Brasileiro–São
745 Paulo. In: Muehe, D. (Ed.), Erosão e Progradação No Litoral Brasileiro. Dieter Muehe (Org.),
746 Brasília, MMA. MMA, Brasília, Brasil, pp. 297–346.
747 Teuten, E.L., Saquing, J.M., Knappe, D.R.U., Barlaz, M.A., Jonsson, S., Björn, A., Rowland, S.J.,
748 Thompson, R.C., Galloway, T.S., Yamashita, R., Ochi, D., Watanuki, Y., Moore, C., Viet,
749 P.H., Tana, T.S., Prudente, M., Boonyatumanond, R., Zakaria, M.P., Akkhavong, K., Ogata,
750 Y., Hirai, H., Iwasa, S., Mizukawa, K., Hagino, Y., Imamura, A., Saha, M., Takada, H., 2009.
751 Transport and release of chemicals from plastics to the environment and to wildlife.
752 Philosophical Transactions of the Royal Society B: Biological Sciences 364, 2027–2045.
753 Thompson, R.C., Olsen, Y., Mitchell, R.P., Davis, A., Rowland, S.J., John, A.W.G., McGonigle,
754 D., Russell, A.E., 2004. Lost at sea: where is all the plastic? Science (1979) 304, 838.
755 Tian, W., Song, P., Zhang, H., Duan, X., Wei, Y., Wang, H., Wang, S., 2023. Microplastic
756 materials in the environment: Problem and strategical solutions. Prog Mater Sci 132, 101035.
757 Tiwari, M., Sahu, S.K., Rathod, T., Bhangare, R.C., Ajmal, P.Y., Pulhani, V., Kumar, A.V., 2023.
758 Comprehensive Review on Sampling, Characterization and Distribution of Microplastics in
759 Beach Sand and Sediments. Trends in Environmental Analytical Chemistry e00221.
760 Turra, A., Manzano, A.B., Dias, R.J.S., Mahiques, M.M., Barbosa, L., Balthazar-Silva, D.,
761 Moreira, F.T., 2014. Three-dimensional distribution of plastic pellets in sandy beaches:
762 shifting paradigms. Sci Rep 4.
763 Van Cauwenberghe, L., Devriese, L., Galgani, F., Robbens, J., Janssen, C.R., 2015. Microplastics
764 in sediments: A review of techniques, occurrence and effects. Mar Environ Res 111, 5–17.
765 Veerasingam, S., Ranjani, M., Venkatachalapathy, R., Bagaev, A., Mukhanov, V., Litvinyuk, D.,
766 Verzhevskaia, L., Guganathan, L., Vethamony, P., 2020. Microplastics in different
767 environmental compartments in India: Analytical methods, distribution, associated
768 contaminants and research needs. TrAC Trends in Analytical Chemistry 133, 116071.
769 Vito, D., Fernandez, G., Maione, C., 2022. A toolkit to monitor marine litter and plastic pollution
770 on coastal tourism sites. Environ Eng Manag J 21, 1721–1731.
771 Wang, C., Zhao, J., Xing, B., 2021. Environmental source, fate, and toxicity of microplastics. J
772 Hazard Mater 407, 124357.
773 Young, A., Elliott, J.A., 2018. Characterization of microplastic and mesoplastic debris in
774 sediments from Kamilo Beach and Kahuku Beach, Hawai'i Risk of Zoonotic Disease from a
775 Wildlife Reservoir View project.
776 Zeng, E.Y., 2023. Microplastic contamination in aquatic environments: an emerging matter of
777 environmental urgency. Elsevier.
778 Zhang, Y.-Q., Lykaki, M., Markiewicz, M., Alrajoula, M.T., Kraas, C., Stolte, S., 2022.
779 Environmental contamination by microplastics originating from textiles: Emission, transport,
780 fate and toxicity. J Hazard Mater 430, 128453.
781 Ziani, K., Ioniță-Mîndrican, C.-B., Mititelu, M., Neacșu, S.M., Negrei, C., Moroșan, E.,
782 Drăgănescu, D., Preda, O.-T., 2023. Microplastics: a real global threat for environment and
783 food safety: a state of the art review. Nutrients 15, 617.
784